

Restructuring and destruction of hydrocarbon dust in the interstellar medium

M. S. Murga,^{1,*} S. A. Khoperskov,^{1,2,3} D. S. Wiebe¹

¹*Institute of Astronomy, Russian Academy of Sciences,
ul. Pyatnitskaya 48, Moscow, 119017 Russia*

²*Università degli Studi di Milano, Dipartimento di Fisica, via Celoria 16, I-20133 Milano, Italy*

³*Sternberg Astronomical Institute, Lomonosov Moscow State University,
Universitetskii pr. 13, 119992 Moscow, Russia*

A model of key processes influencing the evolution of a hydrocarbon grain of an arbitrary size under astrophysical conditions corresponding to ionized hydrogen regions (HII regions) and supernova remnants is presented. The considered processes include aromatization and photodestruction, sputtering by electrons and ions, and shattering due to collisions between grains. The model can be used to simulate the grain size distribution and the aromatization degree during the evolution of HII regions and supernova remnants for a specified radiation field, relative velocity of gas and dust, etc. The contribution of various processes to the evolution of hydrocarbon dust grains for parameters typical for the interstellar medium of our Galaxy is presented. Small grains (less than 50 carbon atoms) should be fully aromatized in the general interstellar medium. If larger grains initially have an aliphatic structure, it is preserved to a substantial extent. Variations in the size distribution of the grains due to their mutual collisions depend appreciably on the adopted initial size distribution. For the MRN initial distribution a significant redistribution of grain sizes is obtained, which increases the mass fraction of smaller grains. Characteristic for an initial distribution from the work of Jones et al. (2013), with high initial fraction of small grains, is a general decrease in the number of grains of all sizes.

* E-mail: murga@inasan.ru

1. INTRODUCTION

Interstellar dust manifests itself as a source of infrared (IR) and submillimeter radiation, as well as a source of absorption in the optical and ultraviolet (UV). One of the most prominent features of the dust emission spectrum is emission bands at wavelengths from 2–20 μm . The origin of these bands is believed to be related to aromatic hydrocarbon compounds. However, it is still unclear in which form they are present in the interstellar medium (ISM). Initially, they were associated with polycyclic aromatic hydrocarbons (PAHs); i.e., planar macromolecules consisting of benzene rings [1, 2]. Recently, it has been also suggested that PAHs or individual benzene rings could be included in a more complex and less ordered structure known as hydrogenated amorphous carbon (a-C:H) [3, 4] or mixed aromatic-aliphatic organic nanoparticles [5]. Such compounds may exist as PAHs in some cases, however, in general, they are not identical to PAHs in their properties (structure, shape, density, heat capacity, absorption cross section, etc.). Each model has its advantages and drawbacks, and the ultimate choice of some specific representation of dust properties is still to be made [6–8].

Whatever compounds are responsible for dust emission in IR bands, observations indicate that their absolute abundance and their abundance relative to larger dust grains vary from galaxy to galaxy [9–11], within a single galaxy [12, 13], within individual HII regions [14], and also change with time [15, 16]. In other words, the observations hint that the evolution of small dust grains (1) differs from the evolution of large dust grains, and (2) is sensitive to parameters of the local ISM (metallicity, velocity field, temperature, etc.). In objects with extreme physical conditions (HII regions, supernova-driven shells), the destruction of dust is efficient [17], while, for example, in dense, cool molecular clouds the opposite process may occur, which is the growth of dust grains by accretion or coagulation [18, 19].

Observations with the Spitzer and Herschel space telescopes have become an important source of information about the properties of the dust component in galaxies and individual star-forming regions (SFRs), in particular, in photometric bands centered on wavelengths of 8 μm and 24 μm . It is generally assumed that the flux in the 8- μm photometric band (F_8) characterizes emission of PAHs, since several bright aromatic emission bands fall into this range, while the 24- μm flux (F_{24}) is associated with emission of larger dust grains. According to a number of studies [13, 20], the flux ratio F_8/F_{24} can be used as a measure of such an important parameter of the dust component as the fraction of aromatic dust grains in the

overall mass of dust (q_{PAH}).

One of well known properties of the dust component emission in SFRs in the near- and mid-IR is the correlation of F_8/F_{24} with the metallicity of the gas, which is usually parameterized through the oxygen abundance, $12 + \log(\text{O}/\text{H})$, in studies of SFRs. Specifically, F_8/F_{24} is lower in objects with lower metallicities (see, e.g., [21]). Various mechanisms have been proposed to explain this correlation, associating the content of metals either with the formation efficiency or the destruction efficiency of the dust grains responsible for the IR emission at 8 and 24 μm .

The hypothesis that the $F_8/F_{24} - 12 + \log(\text{O}/\text{H})$ correlation is associated with different efficiencies of the *formation* of aromatic compounds in stars with different metallicities is not consistent with the local character of this correlation. Essentially, the ratio of IR fluxes correlates with the metallicity of the gas in which aromatic compounds are currently located, not with the metallicity of stars in which these compounds presumably have been synthesized. However, the hypothesis relating a higher rate of *destruction* of aromatic compounds in the low metallicity medium also contradicts to observations. It was shown in [15, 16] that in low metallicity SFRs the F_8/F_{24} ratio grows with age, rather than decreasing with age, as would be expected if the evolution of aromatic compounds was dominated by their destruction. A decrease of this ratio with age is observed only in SFRs having solar or higher metallicity. This suggests that the evolution of small dust grains and macromolecules in SFRs has a complex nature, which is determined by balances between several processes.

Interest to the detailed evolution of dust grains is caused by at least two factors. First, their IR emission is often used as a proxy for the star formation rate. Complicated evolution of dust grains in SFRs could lead to incorrect interpretation of IR observations. Second, the evolution of small hydrocarbon dust grains attracts attention from astrochemical and astrobiological points of view, since it is connected to the survival of organic compounds in the ISM. Moreover, the synthesis of molecular hydrogen may proceed at higher temperatures on surfaces of a-C:H dust grains than on surfaces of “ordinary” dust grains [22].

Studying various aspects of dust evolution requires a model which would take into account both processes of dust formation, growth, and destruction and possible grain structural variations, which are reflected in their IR emission. So far, these processes have been considered separately (see, e.g., [23] and [24]). In the current study, we present a generalized model for the evolution of dust grains, responsible for emission in IR bands, under the action of

processes typical for the ISM, HII regions, and supernova remnants. The model is based on the study [4], which examines the idea that interstellar carbon dust grains consist of amorphous hydrocarbon material, a-C:H, whose structure changes when it is subject to UV irradiation. The ability of these grains to radiate in IR bands is determined by the degree of their aromatization. The optical properties of a-C:H material for various aromatization degrees and the method to calculate the aliphatic to aromatic transition rate are taken from [4]. Unlike the previous models [4, 23, 25], our model includes several evolutionary processes, namely, photodestruction with restructuring, destruction due to collisions with high energy ions and electrons, and destruction due to collisions between the grains themselves. We do not consider dust formation and growth processes in this version of the model, but plan to include them in the future.

One of the key processes included in the model is the restructuring of dust grains illuminated by UV radiation, which forces transition of dust grains from an aliphatic state saturated in hydrogen to a hydrogen-poor aromatic state [4, 26]. This process (called “aromatization” for short) has been often observed in laboratory experiments on Earth [27, 28] and in near-Earth space [29]. Aromatization likely also occurs in the ISM, especially in the presence of enhanced (relative to the average circumsolar background) UV radiation [30–33]. Note that accretion of hydrogen atoms from the ISM could also lead to the opposite transformation from aromatic to aliphatic skeleton [34]. However, the current version of the model is motivated by our wish to study dust in complexes of ionized hydrogen, where high-energy collisions with atomic hydrogen lead to the destruction of dust grains, rather than to the incorporation of atoms into a grain structure.

The destruction of dust grains by high-energy particles (electrons, ions) plays an important role in medium which is dominated by high-velocity ($\gtrsim 10$ km/s) large-scale gas motions or high temperatures ($\gtrsim 10^4$ K). A “molecular” approach to treating the interactions of a carbon lattice with incident particles was developed in [25, 35, 36] for computations of the PAH destruction rate. This approach was adapted for more complex a-C:H dust grains in [37], where the necessity of its use in studies of dust grains with fewer than 1000 atoms is emphasized. For larger dust grains a less detailed “classical” approach can be used, where the efficiency of atom knocking from the grain surface is calculated [38, 39].

High speed collisions between dust grains (>1 km/s) lead to their shattering, which changes the grain size distribution [38, 40]. The efficiency of this process depends on the

properties of turbulent and systematic motions in the medium. Under certain conditions, the fraction of small dust grains can be substantially increased due to the destruction of larger dust grains [41, 42].

In the ISM these various processes compete with each other, and the role of each process depends on specific conditions. Here we present a model of the evolution of the abundance of small hydrocarbon dust in the ISM. Section 2 presents our general approach to describing the evolution of dust. The processes considered are described in detail in Section 3. We analyze the contribution of various processes to the evolution of dust in Section 4. Finally, we formulate our main conclusions in Section 5.

2. GENERAL DESCRIPTION OF THE DUST EVOLUTION

We consider the evolution of a-C:H hydrocarbon dust grains, which initially have an amorphous structure but can be partially aromatized under the action of UV radiation and collisions with gas particles (electrons, ions). There is no separate population of PAHs in the model; they are represented by dust grains with a high aromatization degree. Note that the model can be used to study other dust populations, for example, fully aromatized dust, with appropriate initial conditions.

We used a discrete description of the dust grain population, assuming that their initial size distribution can be described by some arbitrary function $n(a)$, which corresponds to the mass distribution $\tilde{n}(m)$. Shattering due to grain-grain collisions produces dust grains of various masses, causing the function $\tilde{n}(m)$ to change with time. When one uses the distribution of dust grain number per unit mass interval and a limited number of size (mass) bins, the mass conservation can be violated in real computations, for example, when a grain loses only a small amount of mass and remains in the same mass bin, while the associated dust-grain fragment falls into a bin corresponding to a smaller mass. To avoid violation of the mass conservation, we introduced a mass-density function $\tilde{\rho}(m)$, which specifies the total mass of dust grains per unit volume for a mass bin i [41]:

$$\tilde{\rho}_i = \bar{m}_i \tilde{n}_0(\bar{m}_i)(m_i - m_{i-1}), \quad (1)$$

where m_i and m_{i-1} are the bin boundary values and \bar{m}_i is the mean mass of the dust grains

in the bin i :

$$\bar{n}_i = \frac{\int_{m_{i-1}}^{m_i} \tilde{n}_0(m) m dm}{\int_{m_{i-1}}^{m_i} m dm}.$$

Here the subscript 0 denotes the distribution function at the initial time moment. Note that this is not the only way to do this. Violation of mass conservations can also be avoided by normalizing variations in a mass bin to the mean mass in the bin (see [43] for more detail).

A key difference of our model from other similar studies is that we considered dust grains not only of different masses, but also of different aromatization degrees. It is assumed that the degree of aromatization of the dust grains can be described by a wide energy bandgap for the dust material E_{gap} , which reaches a maximum when the dust is fully hydrogenated ($E_{\text{gap}} \sim 3$ eV) and approaches zero in the aromatic state. Therefore, in our model, the mass-density function $\tilde{\rho}$ is a function of two parameters: the mass of dust grains m and the bandgap energy E_{gap} . The number of size (mass) bins is N^a , the number of bins over the bandgap is N^{eg} . The mass distribution of the dust grains allows for various descriptions and normalization. In this study, we characterized the mass using the total number of carbon atoms in the grain, N_{C} .

The time variation of the quantity $\tilde{\rho}_{ij}$ in the mass bin i and the energy bandgap bin j is the sum of the variations due to each of the processes included in the model:

$$\begin{aligned} \frac{d\tilde{\rho}_{ij}}{dt} = & \left[\frac{d\tilde{\rho}_{ij}}{dt} \right]_{\text{arom}} + \left[\frac{d\tilde{\rho}_{ij}}{dt} \right]_{\text{photo}} + \\ & + \left[\frac{d\tilde{\rho}_{ij}}{dt} \right]_{\text{sput}} + \left[\frac{d\tilde{\rho}_{ij}}{dt} \right]_{\text{shat}}, \end{aligned} \quad (2)$$

where the subscripts “arom”, “photo”, “sput,” and “shat” refer to the processes of aromatization, photodestruction, sputtering, and shattering, respectively. The process of aromatization changes the distribution of the dust grains only over E_{gap} , photodestruction changes their mass distribution, and the remaining processes affect the distributions over both of these parameters. Here, we do not follow the mass-density function per se, but rather variations in the number of hydrogen atoms in the dust grain and the degree of its aromatization. We assumed that all the dust grains in a bin ij evolve in the same way. If variations in N_{C} and E_{gap} in a bin give rise to new values of these parameters that correspond to a different bin, all the dust grains are moved to that other bin. In other words, if the parameters of

a bin have changed only insignificantly and remain within the limits for that bin, the mass density of the bin does not change. If the parameters of a bin have changed significantly, the bin with the corresponding values of N_C and E_{gap} is found, and that bin acquires the mass density of bin ij . When considering the process of shattering, the mass-density function was computed directly.

The next section describes the computation of the individual terms in the set of equations (2). The results are presented in the form of the rates R corresponding to the numbers of acts of specific processes per unit time per dust grain.

3. MICROSCOPIC PROCESSES

A dust grain in the ISM is gradually affected by various external influences, which can lead to changes in both its size and its structure. It can lose some of its atoms, fragment into smaller dust grains or into atoms and simple chemical compounds. These variations are mainly due to absorption of photons, as well as due to collisions of dust grains with energetic particles and with each other. These processes have been considered in the literature earlier, but some of them have been studied only in relation to PAHs. Here, we present a corrected approach suitable for “generalized” a-C:H dust grains. Note that the smallest of the dust grains we have considered are essentially macromolecules. In the literature, the term macromolecule is sometimes used to refer to PAHs. In our model, there is no such thing as a “pure” PAH, since PAHs are a subset of a-C:H dust with a continuous size distribution. Therefore, to avoid confusion, we will refer to all the dust particles we have considered as grains. At the same time, for some processes associated with the smallest grains, we apply theories developed for macromolecules, together with the corresponding terminology.

3.1. *Interaction with Radiation*

Photons with energies $E > 3$ eV, i.e., UV photons, exert a significant influence on small dust grains and macromolecules. The absorption of such a photon by a dust grain can have several outcomes — dissociation, radiation, and ionization. The probability that one of these outcomes is realized depends on its activation energy, the photon energy, and the size and composition of the dust grains. In its general form, the rate R (in units of events per second)

for any photoprocess occurring in a grain with radius a under the action of a radiation field $F(E)$ is

$$R(a) = \int_0^{\infty} Y(a, E) C_{\text{abs}}(a, E) F(E) dE. \quad (3)$$

Here, $F(E)$ is the radiation flux written in terms of the number of photons with energy E , Y is the probability of occurrence (yield) of a process upon absorption of a photon with energy E , and $C_{\text{abs}}(a, E)$ is the grain absorption cross section. In our computations we used the optical properties of a-C:H calculated in [44–46]. Further, Eq. (3) was used to take into account the contribution of photoprocesses in the set of equations (2).

The probabilities of breaking a C–H bond and of photoionization are known from experiments and/or theoretical computations (see below). The probabilities for the other processes can be found if the rate constants k_i for all possible processes are known; in our case, this includes radiation, ionization, and breaking of C–C bonds (a sum over these processes is in the denominator, over the subscript j). The probability of the occurrence of process i can be found using the formula

$$Y_i = \frac{k_i}{\sum_{j=1,3} k_j}. \quad (4)$$

Here, we take the rate constant k_i of a process to be its rate in units of events per second, subject to the condition that the probability of obtaining some result is equal to unity.

3.1.1. Aromatization and photodissociation. When modeling photodissociation, we adopted the general scheme presented in [47] for PAHs, extending it to a-C:H dust grains. In this scheme, the partial destruction of a-C:H dust grains can be divided into two stages. First, the main channel is the removal of a hydrogen atom, (dehydrogenation). The bonds with neighboring carbon atoms that are freed after the removal of the hydrogen atom form new bonds, which gradually form a closed ring: the structure of the dust grains makes a transition from an aliphatic to an aromatic state [27, 28]. Laboratory studies of this process are presented in [26–28, 48], and theoretical computations of its rate are described in [49, 50].

Initially, the value of N_C corresponding to the mean mass for a given bin and the constant value $E_{\text{gap}} = 2.67$ eV is assigned to each mass interval. We used the relation $E_{\text{gap}} =$

$4.3X_{\text{H}}$ [49] to estimate the number of hydrogen atoms in a grain, where

$$X_{\text{H}} = \frac{N_{\text{H}}}{N_{\text{C}} + N_{\text{H}}}.$$

During the evolution of the grain, the fraction of C–H bonds (X_{H}) varies, as well as the fraction of aliphatic (X_{sp^3}) and aromatic (X_{sp^2}) C–C bonds. Expressions for calculating X_{sp^3} and X_{sp^2} can be found in [44].

At the *first stage*, the main channel for dissociation is a loss of a hydrogen atom. The cross section for this reaction, $\sigma_{\text{loss}}^{\text{CH}}$, has been measured in a number of experiments [26, 51, 52] for radiation energies from ~ 6 to ~ 22 eV, and varies from 10^{-21} cm $^{-2}$ to 1.5×10^{-19} cm $^{-2}$. We used the mean value $\sigma_{\text{loss}}^{\text{CH}} = 10^{-20}$ cm $^{-2}$ [45] for all photons with energies from 10 to 13.6 eV, and adopted a cross section of zero outside of this range. The probability of dissociation, $Y_{\text{diss}}^{\text{CH}}$, is about 0.1 [53]. The rate at which C–H bonds are broken (and, in our model, the rate of aromatization) per dust grain is

$$\begin{aligned} R_{\text{arom}}(a, E) &= \\ &= \int_{10 \text{ eV}}^{13.6 \text{ eV}} Y_{\text{diss}}^{\text{CH}} \frac{\sigma_{\text{loss}}^{\text{CH}}}{\pi a^2} C_{\text{abs}}(a, E) F(E) dE. \end{aligned} \quad (5)$$

This expression is based on formula (32) from [53]. The upper limit of the integration, 13.6 eV, is justified by the fact that we consider the evolution of dust grains in an “ordinary” ISM, where shorter-wavelength photons are absent. In the vicinity of hot stars, it is necessary to take into account more energetic radiation, and consequently the cross section $\sigma_{\text{loss}}^{\text{CH}}$ for higher energies.

The model assumes that the number of broken bonds is limited by the depth to which a photon penetrates into the dust grain. The maximum penetration depth is assumed to be 200 Å for all dust grains, independent of the photon energy [45]. This means that small dust grains will be aromatized throughout their volume, while grains with radii exceeding 200 Å will be aromatized only in a surface layer.

When the fraction of hydrogen atoms X_{H} becomes less than 5%, the *second stage* ensues, when another dissociation channel is switched on [54, 55] — removal of C_2 . It is suggested in [47] that PAH macromolecules eject acetylene molecules upon photodissociation, but C_2 will likely be removed from fully dehydrogenated dust grains.

Essentially, destruction via the loss of C_2 is efficient only for small dust grains or macromolecules. In particular, it was shown in [47, 56] that the second stage plays an important

role only for macromolecules with less than 50 atoms. The main dissociation channel for larger dust grains is removal of hydrogen atoms [57]. The value of X_{H} required for the onset of the second stage is not reached by such grains.

As in [47], we used the Rice-Ramsperger-Kassel (RRK) approximation [58] adapted for PAHs in [56] to calculate the rates of the removal of an atom or a group of atoms. In this approximation it is assumed that the rate at which an element is removed from a macromolecule with a given number of atoms N_{atom} is related to its internal energy E_{int} :

$$k_{\text{loss}} = k_0(1 - E_0/E_{\text{int}})^{3N_{\text{atom}}-7} \quad (6)$$

with $k_0 = (10^{16}, 10^{16}, 10^{15}) \text{ s}^{-1}$ for H, H₂, and C₂, respectively. It is assumed that the internal energy of a dust grain E_{int} is equal to the energy of the absorbed photon E . Unlike [47, 56], where the region of neutral hydrogen with $E < 13.6 \text{ eV}$ was considered, we extrapolate this expression to higher energies.

The value of E_0 for several small PAHs was obtained experimentally [56], however, it was shown in [35] that this experimental value is not quite appropriate for a mixture of interstellar PAHs, and several values of E_0 were used instead. In our model, this quantity is considered as a parameter.

3.1.2. IR emission. The rate at which IR photons are emitted k_{IR} can be estimated in terms of the absorption cross section C_{abs} [59]:

$$k_{\text{IR}}(E) = \int \frac{C_{\text{abs}}(\lambda)4\pi B_{\lambda}(T[E])d\lambda}{hc/\lambda}, \quad (7)$$

where $T[E]$ is the vibrational temperature corresponding to the energy of the absorbed photon E , $B_{\lambda}(T[E])$ is the Planck function corresponding to the temperature $T[E]$ at wavelength λ , and h and c are the Planck constant and the speed of light. The temperature $T[E]$ can be found if the specific heat capacity of the material C_V is known, which for a-C:H is the sum of the specific heat capacities of the C–H (sp^3) and C–C (sp^2 and sp^3) bonds [4], in proportions corresponding to the relative numbers of these two types of bonds

$$C_V = \frac{1}{1 - X_{\text{H}}} \left[X_{\text{H}}C_V(\text{CH}) + \right. \\ \left. + X_{\text{sp}^2}C_V(\text{CC}_{\text{sp}^2}) + X_{\text{sp}^3}C_V(\text{CC}_{\text{sp}^3}) \right]. \quad (8)$$

We applied this formula to calculate the specific heat capacity, using the technique of [60] for the C–C and C–H aromatic bonds and the experimental data for polyethylene [61] for

aliphatic bonds. The derived heat capacities demonstrate a tendency to grow as the fraction of hydrogen atoms or the bandgap increases [62], so that the temperatures of dust grains of the same internal energy can differ appreciably for hydrogenated and dehydrogenated amorphous hydrocarbon material.

3.1.3. Ionization. The ionization probability function $Y_{\text{ion}}^{\text{V}}$ from [63] was utilized for PAHs in [47], which we adopt as a basis for calculating the rates of various destruction processes. According to this expression, all the energy goes into ionization when the photon energy is $E > 17$ eV. Since photons with such energies were not considered in [63], this choice of an ionization probability function was not of utmost importance for that study. Since we wish to apply our model to studies of the evolution of dust inside HII regions, we instead used the ionization probability function $Y_{\text{ion}}^{\text{WD}}$ proposed for PAHs in [64] to estimate the probability of ionization of the dust grain upon absorption of a photon. This expression makes it possible to model the response of the dust grain to absorption of a hard photon in more detail, admitting both ionization and destruction of the dust grains.

Since photons with energies higher than 17 eV are present only in the vicinities of massive stars, our choice of the ionization probability function is important only for estimating photodestruction rates near such objects. However, in our model, the destruction probability function is also used to calculate the rate of destruction of dust grains due to collisions with high-velocity ions and electrons, which can transfer a substantial energy to a grain, making our choice of Y_{ion} more critical.

3.2. Interactions with Gas

Ions and electrons can also possess kinetic energies sufficient to destroy dust grains with which they collide. The behavior of this interaction differs qualitatively for large and small ($N_{\text{C}} < 1000$) dust grains, which essentially correspond to large molecules. Large dust grains are bombarded by energetic particles only at their surfaces, and are affected only by surface sputtering, while the bombardment of small dust grains can occur throughout their volume, leading to their complete destruction. Two types of interactions between energetic particles and hydrocarbon dust grains can be distinguished: 1) removal of a hydrogen atom or C_2 molecule upon excitation of a dust grain, 2) direct removal of an atom from the lattice due to a collision. A description of the interactions of small and large dust grains with gas adopted

in our model is presented below.

3.2.1. Statistical sputtering of small dust grains. Here, statistical sputtering refers to the dissociation (removal) of a structure element of a dust grain as a result of de-excitation following the absorption of the energy of an incident particle when it interacts with the electron cloud of the dust grain. This type of collision is also referred to as an inelastic collision. As a whole, the situation is similar to the absorption of a photon, but in this case, the kinetic energy of the incident particle can be transferred to the lattice only partially. Only charged particles exert a substantial influence in statistical sputtering; i.e., only ions and electrons. Neutral atoms do not interact with the electron cloud of a dust grain, and can act on the lattice only when they impact one of its nodes directly.

The transferred energy E_{tr} depends on the efficiency of the friction experienced as the particle moves inside the dust grain and the distance traversed. Computations of these quantities were carried out for PAHs in [35]. Here, we used analogous computations with changes related to the different geometry of the dust grains considered. We assume that the molecular structure of an a-C:H dust grain can be represented by a cube consisting of N_p layers, each of which is a quasi-PAH [37] (of course, real a-C:H dust grains are unlikely to have such a simple shape). In this geometry, the total number of layers in the grain can be estimated as $\sqrt[3]{N_C - 1}$. Each layer contains $N_C^p = (N_C)^{2/3}$ atoms. Passing through one layer, an ion transfers an energy E_{tr}^0 to the grain, which can be calculated as described in Appendix A. The total energy transferred by the ion to the a-C:H grain, E_{tr} , will be $N_p \times E_{\text{tr}}^0$ if the ion passes through the whole grain, and $N_l \times E_{\text{tr}}^0$ if the number of layers traversed by the ion $N_l = E_{\text{ion}}/E_{\text{tr}}^0$ is less than N_p .

The processes occurring in the grain as a result of such absorption of energy were treated analogously to the absorption of a photon, with E_{int} in (6) replaced by E_{tr} . If the dust grains are hydrogenated, this energy (taking into account the dissociation probability $Y_{\text{diss}}^{\text{CH}}$) will go into the removal of hydrogen atoms and aromatization. In the case of dehydrogenated grains, dissociation occurs via the loss of C_2 molecules.

Taking into account all possible arrival directions of the ions (the angle θ), the rate at which dust grains are destroyed as a result of statistical sputtering by ions $R_{\text{s}}^{\text{ion}}$ can be

calculated using the formula

$$R_s^{\text{ion}} = v_{\text{ion}} n_{\text{ion}} \int_0^{\pi/2} \sigma_g Y[E_{\text{tr}}(\theta)] \sin \theta d\theta, \quad (9)$$

where n_{ion} is the number density of ions in the medium and σ_g is the geometrical cross section of the a-C:H dust grains. This must be multiplied by two to take into account destruction due to the removal of C₂ groups. Note that, when considering interactions of an ion with a dust grain, the charge of the grain must also be taken into account in the Coulomb factor, but we have not concerned ourselves with this issue, since we assume that all the dust grains are neutral. In fact, the grain charge can substantially influence some microprocesses; for example, it can play an important role in the dynamics of dust in HII regions and shocks [65, 66], by determining the relative velocity of the dust grains and gas. However, in our case, introducing a grain charge would mean considering a three-dimensional rather than two-dimensional distribution of the dust grains, which appreciably complicated the computations. Since the collisional velocities in this study are specified and not derived from a physical model, the only error introduced by assuming the dust grains are neutral is associated with the Coulomb factor.

Formula (9) can be used for a specific value of velocity of an incident ion v_{ion} , for example, due to non-thermal gas motions. When thermal motion of the ions is considered, we must integrate over all possible velocities:

$$R_{s,T}^{\text{ion}} = 2 \int_{v_{\text{ion}}^0}^{\infty} R_s^{\text{ion}} f(v_{\text{ion}}, T_{\text{gas}}) dv_{\text{ion}}, \quad (10)$$

where $f(v_{\text{ion}}, T_{\text{gas}})$ is a Maxwellian distribution for given ions at a temperature T_{gas} and v_{ion}^0 is the speed corresponding to the minimum energy required for dissociation, estimated using (9).

Incident electrons can also interact with the electron cloud of a dust grain. The electrons in a hot gas can reach kinetic energies of several tens or even hundreds of eV, which can lead to the destruction of a dust grain during a collision. To estimate the energy E_{tr}^e obtained from an electron, one needs to calculate the Mott cross section [67], which is a laborious task. It was proposed in [35] to use the experimental approximation from [68], obtained for graphite, for this cross section. We used the algorithm of [35] to compute E_{tr}^e , which is taken to be the difference between the initial energy of the electron E_0^e and its energy

after it has passed through a PAH, E_1^e , which is found taking into account the traversed distance. This distance was estimated in the same way as that for an ion (Eq. A2). The energy is also multiplied by a factor of N_l to take into account the volume of the a-C:H dust grain. We then calculated the probability of the removal of a C_2 group and found the rate of destruction of dust grains by electrons using formula (10), replacing the subscript and superscript “ion” with “e”. Due to the low mass of the electron, with typical velocities for large-scale motions in the ISM, the influence of non-thermal collisions is negligible, and we have accordingly taken into account only thermal collisions.

3.2.2. Non-statistical sputtering of small dust grains. Non-statistical sputtering refers to the removal of atoms from the lattice of dust grains as a result of interactions between the nuclei of atoms in the lattice and an incident ion with a kinetic energy exceeding the binding energy of the atoms to the lattice.

In the computations of the destruction efficiency in [25], elastic collisions between particles (hydrogen, helium, carbon) moving with a velocity v_{ion} and stationary carbon atoms in the lattice are considered. As a result of a collision, some fraction of the kinetic energy of the incident particle is transferred to a carbon atom. If the acquired energy exceeds the critical energy for removing the atom from the lattice (E_{crit}), the dust grain will lose an atom. The value of E_{crit} can be estimated only approximately, first, due to the lack of reliable experimental data and second, because this quantity most likely depends on the size, structure, and charge of the dust grain, as well as the position of the atom in the lattice: atoms at the edge of the grain can be removed much more easily than atoms in the central part of the grain. In our model, we adopted the value $E_{\text{crit}} = 7.5$ eV, as was done in [25] for PAHs. Generally speaking, we consider not PAHs, but rather compounds that could include both aliphatic and aromatic bonds. Since aliphatic bonds are not as strong as aromatic bonds, the kinetic-energy threshold could be lower for the former. However, as a rule, a molecular treatment of the bombardment process is only important for very small dust grains, which rapidly aromatize, as was noted above. Accordingly, their bonds are to a large extent aromatic.

Such collisions are described in [25] using the Ziegler-Biersack-Littmark (ZBL) theory [69], which can be used to find the energy $\langle E_{\text{tr}}^{\text{elas}} \rangle$, transferred to a carbon atom by an incident particle, as well as the interaction cross section σ . The main formulas are presented in Appendix B. Further, we can calculate the collision rate for a single atom in the lattice. For

a flux of ions moving perpendicular to the lattice, this collision rate can be calculated as

$$R_{n,0}^{\text{ion}} = n_{\text{ion}} v_{\text{ion}} \sigma. \quad (11)$$

To calculate the collision rate for the dust grain as a whole, we must multiply the rate $R_{n,0}^{\text{ion}}$ by the number of possible collisions. Because multiple collisions between an incident particle and atoms in the lattice are possible in bulky grains, the destruction rate can be increased appreciably compared to the destruction rate for a flat structure (PAH). If the energy of the incident ion is sufficient to knock out an atom from the first layer, its energy decreases by $\langle E_{\text{tr}}^{\text{elas}} \rangle$. Our calculation of the energy $E_{\text{tr}}^{\text{max}}$ transferred to the atom in a head-on collision is described in Appendix B. The quantity $\langle E_{\text{tr}}^{\text{elas}} \rangle$ is the energy $E_{\text{tr}}^{\text{max}}$ averaged over all possible arrival angles for the ion. In the second layer, the ion carries the energy $E_0^{\text{ion}} - \langle E_{\text{tr}}^{\text{elas}} \rangle$. If this residual energy is again sufficient to knock out atom, the second layer will also lose an atom from its lattice. This process will continue until the ion leaves the dust grain or its remaining kinetic energy becomes too small to remove another atom. The number of collisions leading to the removal of an atom N_{col} can be estimated as $\min(E_0^{\text{ion}} / \langle E_{\text{tr}}^{\text{elas}} \rangle, N_p)$. The rate of destruction of a-C:H dust grains is then given by

$$R_n^{\text{ion}}(v_{\text{ion}}) = N_{\text{col}} N_C^p R_{n,0}^{\text{ion}}. \quad (12)$$

In the case of thermal motion of the gas, we must integrate this destruction rate over the full range of velocities, as in the case of statistical destruction [Eq. (10)]. As was already noted, the most abundant ions are ions of hydrogen and helium; therefore, we consider the destruction caused by these ions for both statistical and non-statistical sputtering, together with carbon ions being representative of heavier ions.

3.2.3. Sputtering of large dust grains. As was shown in [37], the interactions between the lattice and incident particles does not need to be considered in detail in the case of large dust grains ($N_C > 1000$), so that we can restrict our treatment to a classical description of this process. If an atom at the surface of a dust grain acquires sufficient energy during a collision with an incident particle to break its bonds, it leaves the grain. The efficiency of this process has been calculated in multiple studies, for several astrophysically important materials, including graphite and amorphous carbon [38, 40, 70]. The probability of ejecting an atom from the surface Y_{sput} for a-C:H dust grains was calculated in [39]. It was shown that the sputtering rate for a-C:H was higher than for graphite due to its lower density and

the deeper penetration of the ions. It was also found that the degree of aromatization does not influence the sputtering process. We used the Y_{sput} value obtained in [39] for H^+ and He^+ using the Stopping and Range of Ions in Matter (SRIM) program [69]). The rate of sputtering of dust grains with radius a bombarded by ions with velocity v_{ion} can be calculated as

$$R_{\text{sput}}^{\text{nt}} = 2\pi a^2 \sum v_{\text{ion}} n_{\text{ion}} Y_{\text{sput}}^{\text{ion}}. \quad (13)$$

In the case of thermal sputtering, this rate is calculated for the entire range of possible velocities [Eq. (10)]. According to [39], this rate should be multiplied by four to take into account the influence of the arrival angle of the ion.

3.3. Shattering

The last process we consider is collisions between dust grains that lead to their fragmentation into smaller grains. Depending on the velocity of the collision, a dust grain can be destroyed partially or completely. The size and number of fragments must be calculated for each collision. A theoretical description of this process and its application to a number of astrophysical objects are presented in [38, 40–42]. Below we summarize the main assumption of the theory used in our model.

It is assumed that a grain P with mass m_{P} collides with another grain T with mass m_{T} ($m_{\text{P}} \leq m_{\text{T}}$) with the relative velocity of v_{col} . As a result of their collision, grain P is completely destroyed, regardless of its mass. The mass fraction $M_{\text{sh}}/m_{\text{T}}$ of the dust grain T through which the shock generated by the collision passes can be estimated for a given collision velocity and dust material using formulas from [40, 41]. Like the authors of those studies, we assumed that, if M_{sh} comprises more than half of the mass of the dust grains m_{T} , the grain is completely destroyed. Otherwise, the fraction $M_{\text{shat}} = 0.4M_{\text{sh}}$ is fragmented into smaller dust grains. The fragments of both dust grains have power-law size distributions:

$$n_{\text{shat}} = C a_{\text{shat}}^{-3.3} \quad (14)$$

where the factor C can be found from the normalization.

To calculate the parameters of the forming fragments, we must take into account all possible collisions between grains of various sizes and types. In this study, we considered

collisions between hydrocarbon dust grains of various sizes and degrees of aromatization, excluding collisions with silicate grains for the moment (their contribution will be considered in future studies).

Our model comprises N^a dust size bins and N^{eg} bins of the bandgap E_{gap} ; therefore, $N^a \times N^{\text{eg}}$ types of collisions are possible. The size (mass) distribution of the fragments is described above. The distribution of the degree of aromatization of the fragments is estimated as follows. If a dust grain has a radius smaller than 200 Å, i.e., it is uniform in terms of its degree of aromatization, its fragments remain in the same E_{gap} bin as the initial dust grain. If a dust grain has a radius of more than 200 Å, it consists of two layers — an inner layer with the initial degree of aromatization and an outer layer whose degree of aromatization corresponds to the current E_{gap} bin. If the mass fraction of the destroyed material is lower than the mass fraction of the outer layer (with thickness 200 Å), the fragments are assigned the E_{gap} value of the surface layer. Otherwise, the fragments are distributed among the bins with the E_{gap} values for the inner and outer layers, assuming that the outer layer was completely destroyed and the remaining fragments have the E_{gap} value of the inner layer.

The numerical rate of variation of the mass density of a bin as a result of shattering of the dust grain can be expressed as

$$\begin{aligned} \left(\frac{d\tilde{\rho}_{ij}}{dt} \right)_{\text{shat}} &= -\bar{m}_i \tilde{\rho}_{ij} \sum_{j_1=1}^{N^{\text{eg}}} \sum_{k_1=1}^{N^a} \alpha_{ik_1} \tilde{\rho}_{k_1 j_1} + \\ &+ \sum_{j_1=1}^{N^{\text{eg}}} \sum_{j_2=j_1}^{N^{\text{eg}}} \sum_{k_1=1}^{N^a} \sum_{k_2=k_1}^{N^a} \alpha_{k_1 k_2} \tilde{\rho}_{k_1 j_1} \tilde{\rho}_{k_2 j_2} m_{k_1 j_1 k_2 j_2}^{\text{shat}, i, j} \\ \alpha_{k_1 k_2} &= \frac{\sigma_{k_1 k_2} v_{k_1 k_2}}{\bar{m}_{k_1} \bar{m}_{k_2}}, \end{aligned} \quad (15)$$

where $m_{k_1 j_1 k_2 j_2}^{\text{shat}, i, j}$ is the mass of the fragments falling in the bin (i, j) during a collision of dust grains from bins (k_1, j_1) and (k_2, j_2) and $\sigma_{k_1 k_2}$ is the collision cross section for dust grains with masses from bins k_1 and k_2 (determined as $\pi(a_{k_1}^2 + a_{k_2}^2)$). The method used to calculate m^{shat} was taken from [41]. After taking into account all collisions, the degree of aromatization in the bin is calculated as the mean-weighted degree of aromatization of all fragments in the bin, where the mass density acts as the weighting factor.

The process of aromatization does not change the mass of dust grains, and accordingly does not change the number of dust grains in a given mass interval. However, shattering

leads to the transfer of dust grains from a given bin to bins with different aromatization degrees.

4. CONTRIBUTION OF VARIOUS FACTORS TO AROMATIZATION AND DESTRUCTION OF DUST

In this section, we present illustrative computations of variations of the main characteristics of hydrocarbon dust grains under various conditions characteristic for the ISM. Since our main interest is in the IR emission of aromatic compounds, we begin with a computation of the aromatization of dust grains under the action of UV radiation, which leads to the removal of hydrogen atoms. Figure 1 presents the evolution of the width of the bandgap E_{gap} for dust grains with various numbers of carbon atoms N_C , located in radiation fields with various intensities. We assume that the spectrum is a multiple the radiation field estimated in [71] and use a dimensionless coefficient U equal to unity in the vicinity of the Sun as a measure of radiation intensity. We did not take into account the second stage of dissociation in these computations. Note that the shape of the spectrum will be different in SFRs, which are a main potential target for studies using this version of our model, and the model makes it possible to take this into account. However, in this study, we used a parametrization of the spectrum for the vicinity of the Sun for illustrative purposes, and also to enable comparison with the results of previous studies.

Small dust grains with $N_C < 2 \times 10^4$, corresponding to radii less than 35 Å, lose essentially all their hydrogen atoms in several hundred thousand years, even when the radiation field illuminating them is not very strong ($U = 1$). Consequently, there should be no small, hydrogenated, carbon dust grains in the “ordinary” ISM, since they are very rapidly transformed into aromatic grains. The restructuring of larger dust grains takes longer: when $N_C \sim 2 \times 10^4$ (a radius of about 75 Å), the aromatization time is nearly a million years. However, they are also most likely in a dehydrogenated state in the ISM. Dust grains with $N_C > 2 \times 10^5$ ($a > 200$ Å) evolve over long times, and remain predominantly hydrogenated. Increasing the strength of the radiation field by a factor of ten ($U = 10$) allows for appreciable aromatization of larger dust grains on time scales less than a million years. Such radiation fields (and more intense fields) are characteristic, for example, for HII complexes, whose lifetimes comprise several million years. Thus, large dust grains in these objects could

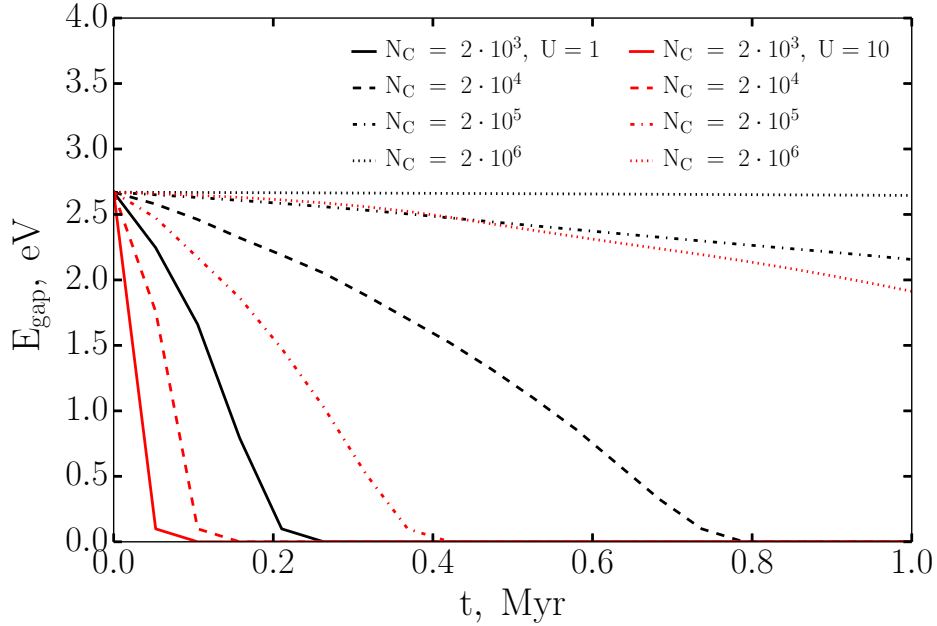


Figure 1. Variation of the width of the bandgap E_{gap} under the action of a radiation field for a-C:H dust grains with various numbers of carbon atoms N_C . Results are presented for radiation fields with $U = 1$ (black) and $U = 10$ (red).

be partially aromatized.

In Figure 2 we compare the probabilities for removal of a C_2 group for various ionization probability functions and for dust grains with various numbers of carbon atoms. The plots for $Y_{\text{ion}}^{\text{V}}$ are shown in red, and those for $Y_{\text{ion}}^{\text{WD}}$ are shown in black. When the function $Y_{\text{ion}}^{\text{WD}}$ is used, dust grains with 16 and 48 atoms are efficiently destroyed at photon energies more than ~ 15 eV, while the destruction of dust grains with 128 atoms begins only for photon energies greater than 17 eV. When the function $Y_{\text{ion}}^{\text{V}}$ is used, which assumes that the energy of the absorbed hard photons goes completely into ionization, the destruction of dust grains with 16 or more atoms becomes inefficient at photon energies of about 17 eV, which seems unrealistic. Moreover, this assumption contradicts recently published experimental results [72], according to which ionization dominates for photon energies from 8 to 40 eV only for large dust grains, while a more important channel for small dust grains is their dissociation (loss of a hydrogen atom).

As was noted above, at the second stage of photodissociation the rate of destruction of dust grains strongly depends on the parameter E_0 . Figure 3 shows the dependence of the

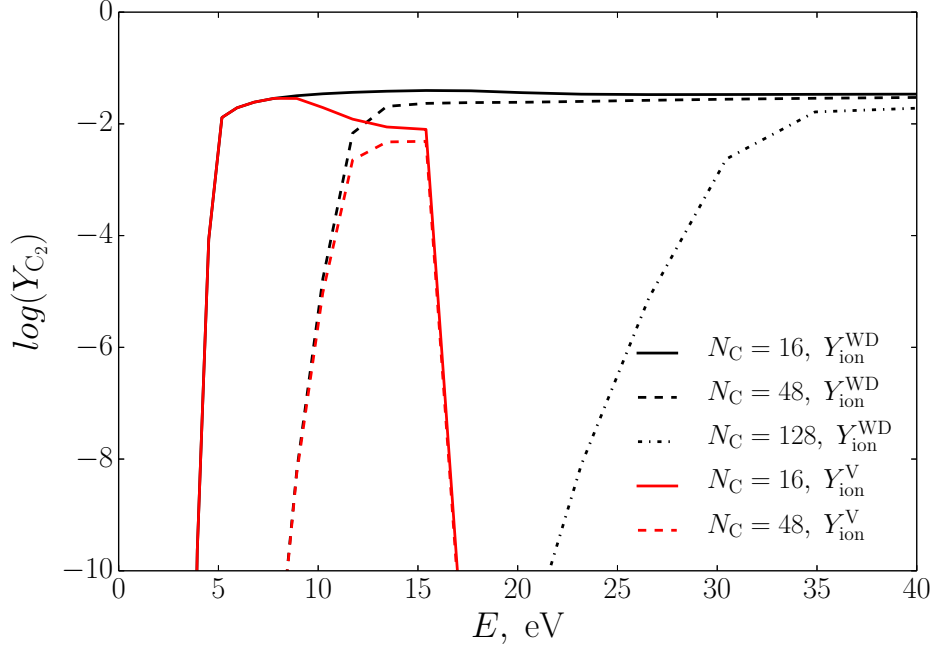


Figure 2. Dependence of the probability of destruction of dust grains with numbers of carbon atoms 16, 48, and 128 for the ionization probability functions $Y_{\text{ion}}^{\text{WD}}$ (black) and $Y_{\text{ion}}^{\text{V}}$ (red).

probability for the removal of a C_2 group (Y_{C_2}) on E_0 for dust grains with $N_{\text{C}} = 16, 28$ and 48 that absorb photons with energies of 8 and 12 eV. The probability of dissociation falls off strongly with increasing E_0 . For the same dust grain that absorbs a photon with energy 12 eV, the probabilities of losing a C_2 group for $E_0 = 3$ and 5 eV differ by five orders of magnitude. It is obvious that computations of the evolution of ensembles of dust particles in SFRs must consider various values for this parameter.

The rate of destruction of a-C:H dust grains calculated using formula (5) is shown in Figure 4 for $E_0 = 2.9$ eV (black) and $E_0 = 5$ eV (red). As E_0 is decreased, a grain with $N_{\text{C}} \sim 50$ can be destroyed by a radiation field with $U = 1$ at a rate of about 10^{-11} carbon atoms per second; i.e., about 3×10^{-4} C_2 groups are dissociated in a year, and the entire dust grain will be destroyed over about 80 000 yrs. However, the destruction rate falls rapidly with increase in the number of atoms. For example the complete destruction of dust grains with $N_{\text{C}} \sim 60$ requires about 10 million years. Thus, when $E_0 = 2.9$ eV, dust grains with more than 50 atoms are stable, and can survive over the characteristic lifetime of an HII complex. If we adopt higher values for E_0 (5 eV), photodestruction becomes unimportant. Even molecules with 20 atoms will be destroyed in a radiation field with $U = 100$ only after

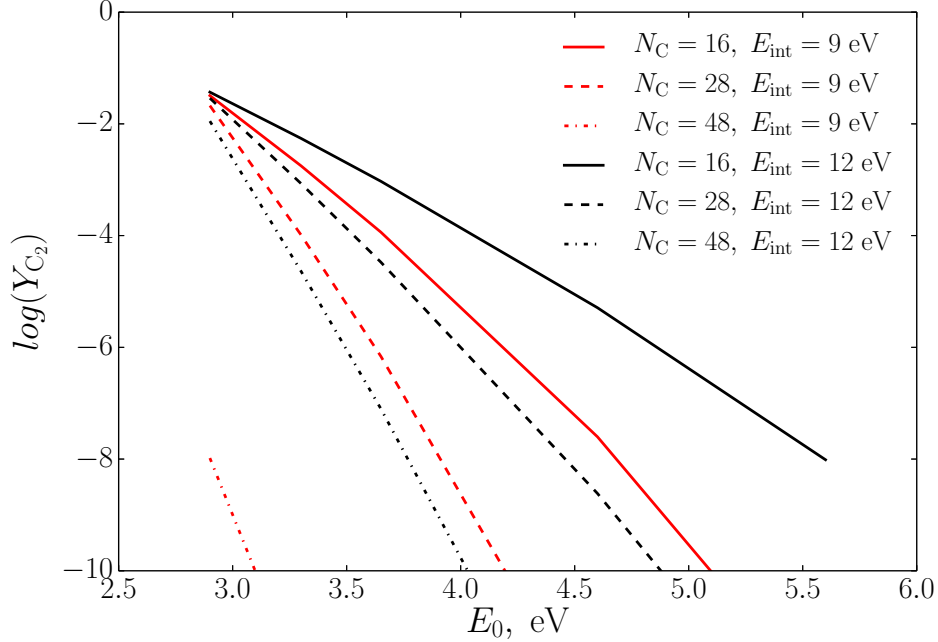


Figure 3. Dependence of the probability of removing a C_2 group on the parameter E_0 characterizing the energy for breaking the C–C bonds. Computations are shown for dust grains with numbers of carbon atoms 16, 28, and 48 (solid, dashed, and dot-dashed lines, respectively) for internal energies of 9 eV (red) and 12 eV (black).

a million years. Such high values of U are not generally characteristic of HII complexes, but the intensities of the radiation fields inside individual HII regions can exceed the radiation field in the solar vicinity by a factor of tens or hundreds of thousands; photons beyond the Lyman limit are also present in HII regions, suggesting that photodestruction can also play a key role in these objects with higher values of E_0 .

These estimates are in agreement with the results of other studies. For example, Allain et al. [47] concluded that photodestruction plays a role in the circumsolar radiation field only for PAHs with fewer than 50 atoms. The critical number of carbon atoms estimated in [56] is about 30–40. Our results are in agreement with these estimates, but we must recall that the critical number of atoms depends strongly on the adopted value of the dissociation energy E_0 .

The role of statistical disruption by non-thermal (left) and thermal (right) particles is illustrated in Figure 5, which presents the computational results in the form of relative decrease in the number of carbon atoms in a dust grain per second. Ions of the most

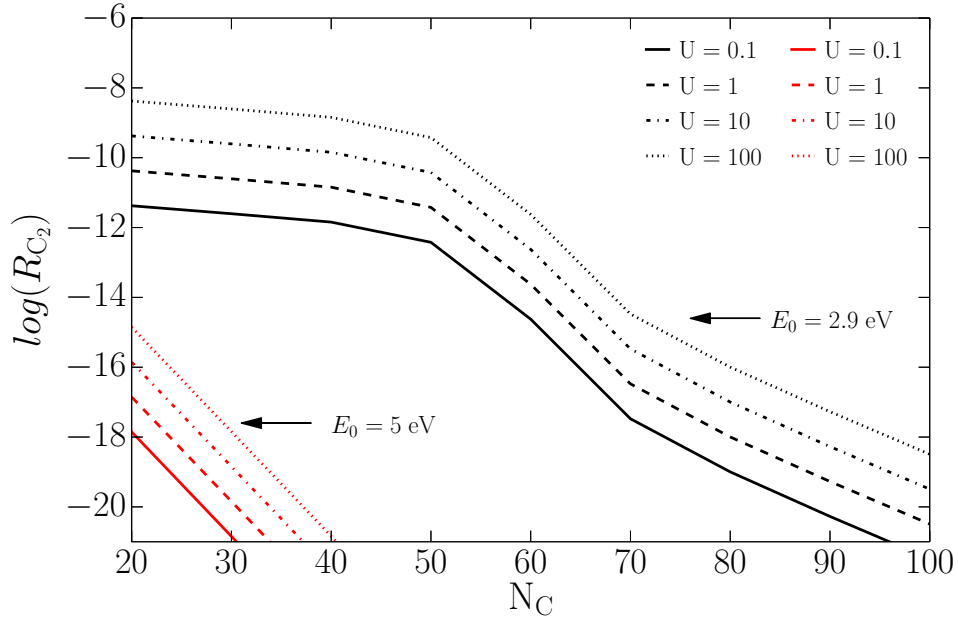


Figure 4. Dependence of the rate of photodestruction of dust grains via the removal of a C_2 group on the number of carbon atoms. Results are presented for radiation fields with $U = 0.1, 1, 10$, and 100 and for $E_0 = 2.9$ eV (black) and 5 eV (red).

abundance elements — hydrogen and helium — are considered, as well as carbon ions as a representative of the population of heavier ions. These computations assumed the following number densities: $n_{H^+} = 1 \text{ cm}^{-3}$, $n_{He^+} = 0.1 \text{ cm}^{-3}$, and $n_{C^+} = 10^{-4} \text{ cm}^{-3}$. It is obvious that with these number densities and $E_0 = 2.9$ eV, collisions at velocities lower than ~ 20 km/s are not sufficient to destroy any dust grains. Formally, carbon ions dominate at these velocities, but the relative decrease in atoms over 10^6 yrs does not exceed 0.1, even for the smallest dust grains.

The destruction of small dust grains by helium ions dominates at velocities from 20 to 50 km/s, leading to a relative decrease in the number of atoms of order 10^{-1} over 10^3 yrs. At velocities above 50 km/s, small dust grains are destroyed mainly by hydrogen ions. Increasing the velocity of collisions with H^+ ions to 100 km/s leads to the destruction of dust grains with $N_C = 25$ over less than 10^3 yrs. Taking into account the fact the enhanced densities in shock fronts, where n_H can reach 10^4 cm^{-3} , the destruction time can be shortened to ~ 0.1 year. The rate of destruction of dust grains with large numbers of atoms ($N_C = 75$) is approximately an order of magnitude lower than the rate for dust grains with $N_C = 25$.

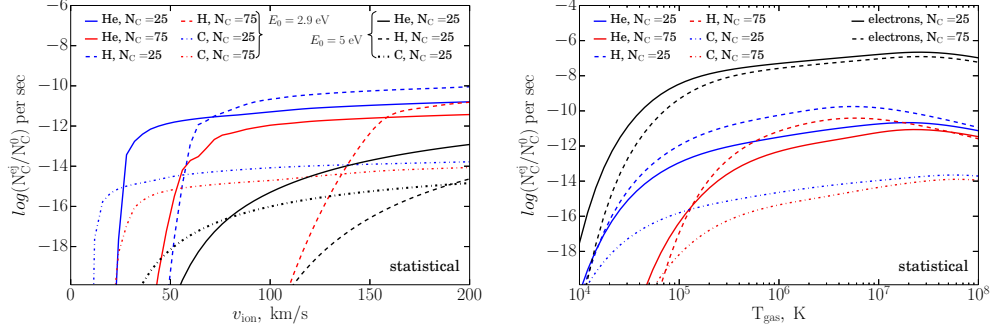


Figure 5. Dependence of the rates of statistical sputtering of dust grains on the velocity of a collision with non-thermal ions (left) and the gas temperature (right). Left: collision of a dust grain with $N_C = 25$ and an ion of hydrogen (blue dotted), helium (blue solid), and carbon (blue dot-dashed) with $E_0 = 2.9$ eV. The corresponding set of lines in red shows the analogous results for a collision with a dust grain with $N_C = 75$, also for $E_0 = 2.9$ eV. The corresponding set of lines in black shows the analogous results for a collision of a dust grain with $N_C = 25$, but for $E_0 = 5$ eV.

Right: blue and red curves show results for collisions of the same dust grains and ions for $E_0 = 2.9$ eV, but for thermal ions. The black solid and dashed curves denote the rates of destruction of dust grains with $N_C = 25$ and 75 , respectively, by thermal electrons.

If we adopt $E_0 = 5.0$ eV, the minimum velocity required for destruction, v_{ion}^0 , increases by about a factor of two, while the destruction rate decreases by several orders of magnitude. For example, with a collision velocity of 100 km/s, the destruction of dust grains with $N_C = 25$ requires no less than 10^7 yrs at the given number density, with the main role in the sputtering of dust grains being played by helium ions.

Figure 5 (right) shows the destruction of dust grains by thermal ions and electrons. Destruction by electrons dominates over destruction by ions at all the temperatures considered. When the temperature of the ambient gas is 10^5 K or more, dust grains with both 25 and 75 carbon atoms are destroyed in about a year. The rate of destruction by thermal ions of a gas at such temperatures is comparable with the rates of destruction by non-thermal ions with collision velocities of order 100 km/s. Non-thermal ions of hydrogen and helium play an important role in the destruction of dust only if the gas temperature does not exceed 10^4 K. At such high temperatures, the dust grains are predominantly destroyed by collisions with thermal electrons. This type of destruction is most important in supernova remnants and, more general, in the hot phase of the ISM. The turbulent velocity dispersion in SFRs

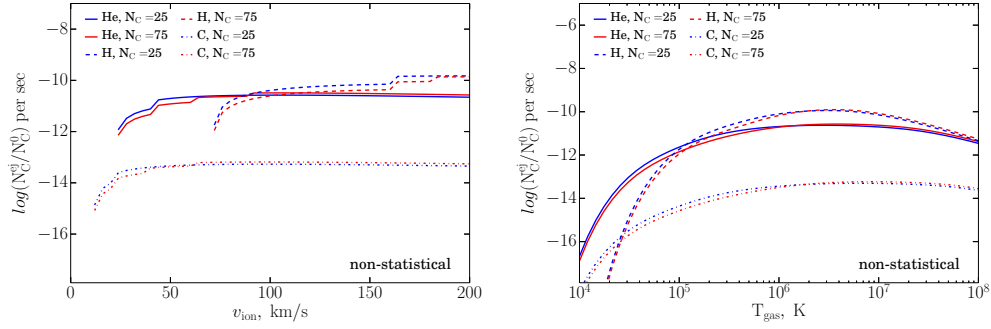


Figure 6. Dependence of the rates of non-statistical sputtering of dust grains on the velocity of collisions with non-thermal ions (left) and on the gas temperature (right). Left: collisions of a dust grain with $N_C = 25$ and ions of hydrogen (blue dashed), helium (blue solid), and carbon (blue dot-dashed). The corresponding set of lines in red shows the analogous results for collisions of dust grains with $N_C = 75$. Right: the blue and red curves denote collisions of the same dust grains and thermal ions.

does not exceed several tens of km/s, and the maximum temperatures near massive stars can reach several thousand Kelvin. Under these conditions, statistical sputtering will always be less efficient than photodestruction.

Figure 6 presents the results of our computations of the rate of destruction of dust grains by non-statistical sputtering. At low velocities (to 70 km/s), the main role is played by helium ions, while collisions with hydrogen ions are also important at higher velocities. Due to their lower abundance, carbon ions play virtually no role. The rates of destruction of dust grains with 25 and 75 atoms are virtually the same, in contrast to the case of statistical destruction; at high velocities, the destruction rate is even higher for larger dust grains. This is expected because the cross section for interaction (the cross section of the dust grains) increases with their size, raising the probability of an incident particle collision with one of the atoms in the lattice.

In contrast to statistical destruction, the rates of this interaction are significant at low velocities: helium ions are capable of destroying a grain with $N_C \leq 75$ after 10^3 yrs, even with collision velocities of the order of 50 km/s. At higher velocities, the destruction rates by ions of hydrogen and helium for elastic and inelastic interactions become comparable. This is also true for thermal ions: at temperature above 10^5 K, the destruction rate by ions is several orders of magnitude lower than the rate of statistical destruction by thermal

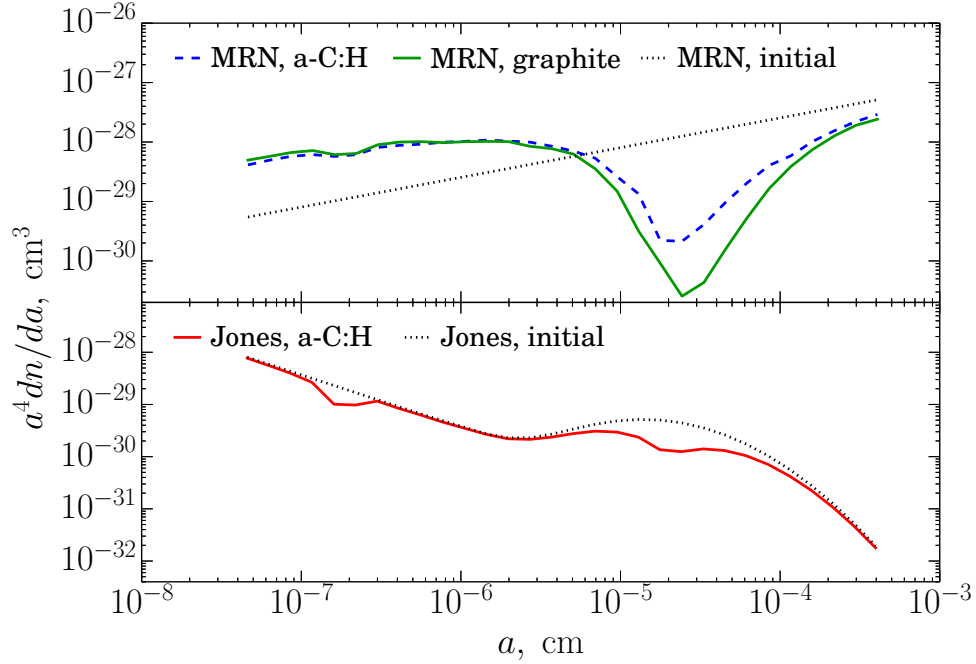


Figure 7. Upper: size distribution of dust grains up to the onset of shattering (black dotted curve) and after one million years, for an MRN distribution. The green curve shows the distribution for graphite grains, and the blue curve the distribution for a-C:H dust grains. Lower: same plot for the initial size distribution taken from [4] and a-C:H dust grains.

electrons.

Finally, let us consider the modeling results for the shattering of dust grains. Figure 7 (top) shows the evolution of the size distribution of the dust grains for an initial MRN distribution [73], extended toward small dust grains to a radius of 4 \AA and toward large dust grains to a radius of $0.4 \text{ }\mu\text{m}$, as was done in [41]. The velocity dispersion of the dust grains was taken from [74] for the case corresponding to a thermal ionized medium. For comparison, in addition to amorphous a-C:H dust grains, the upper panel in Figure 7 also shows the evolution of the size distribution for graphite dust grains. The shattering parameters for these materials are different, and the redistribution of the dust-grain sizes for the two types of grains proceeds differently. The reduction in the number of large dust grains is more efficient for graphite, but this does not significantly affect the increase in the number of small dust grains.

Figure 7 (bottom) presents an analogous computation for an initial size distribution of the dust grains taken from [4]. The redistribution of sizes is less efficient in this case. In

particular, instead of a growth in the number of small dust grains, to some extent, the destruction of dust grains of all sizes is observed. This occurs mainly due to the initially high abundance of small dust grains, whose collisions lead to their total destruction. There are more large than small dust grains in the MRN distribution, so that the destruction of small dust grains is compensated by the shattering of large dust grains. The size distribution from [4] is characterized by the opposite relationship between the numbers of large and small grains, so that the destruction of small dust grains is not balanced by the appearance of fragments of large dust grains. Thus, the chosen size distribution is an important factor in modeling the evolution of dust, and determines the trend in the variation of the abundance of small dust grains.

5. DISCUSSION AND CONCLUSION

Problems related to the destruction of dust grains of various sizes and chemical compositions have been discussed many times in the literature. The novelty of the model presented here is that we have considered not only the destruction of hydrocarbon dust grains of various sizes, but also variations in their structural properties. This latter element is important for modeling the IR radiation of dust grains in the ISM and SFRS. Let us briefly summarize the main characteristics of our model. In the version presented here, we have assumed that hydrocarbon dust grains in SFRs initially (after their formation in asymptotic giant branch stars or molecular clouds) have predominantly aliphatic structure. Interactions of dust grains with UV radiation and energetic particles in the ambient gas leads to a gradual loss of hydrogen atoms and, thus, to the formation of aromatic bonds, either in the entire volume of the dust grain (if its radius is less than 200 \AA), or in a surface layer with a thickness of 200 \AA .

We have considered each of these processes in detail, and have computed the rates of the destruction (or restructuring) of dust for various parameters. We have shown that the aromatization time for dust grains with $N_C < 2 \times 10^3$ is less than 2×10^5 yrs, even for a moderate interstellar radiation field ($U = 1$), so that small dust grains should be fully aromatized in the ISM.

When the fraction of hydrogen atoms in a grain becomes less than 5%, the loss of C_2 , and possibly C_2H_2 , molecules is added to the removal of hydrogen atoms. As a result, such

grains are not only aromatized, but also destroyed. For characteristic evolutionary times in SFRs, the second phase occurs only for small dust grains with less than 50 carbon atoms. Larger dust grains will be affected by this process only in the vicinities of hot massive stars.

Other destruction mechanisms associated with collisions of dust grains and energetic gas particles are efficient only in the case of high collision velocities and/or high gas temperatures. At temperatures above 10^5 K, the main mechanism for the destruction of small dust grains becomes inelastic interactions with thermal electrons.

Finally, an important process leading to a redistribution of the dust-grain sizes is shattering as a result of collisions between dust grains. This process is the main channel for compensating the destruction of small dust due to interactions with photons and sputtering.

We have shown that the evolution of hydrocarbon dust grains of various sizes in the ISM is expressed through variations of their size distribution and structural properties, which should lead to variations in their optical properties [45, 46]. These variations will inevitably be reflected in the emission and absorption properties of the dust component of the ISM. Important applications of the model we have presented include studies of variations of the ratio of the intensities of the emission bands at $3.3\ \mu\text{m}$ and $3.4\ \mu\text{m}$, which may reflect the relative abundance of aromatic and aliphatic hydrocarbons, and explaining the metallicity dependence of the ratio of the 8 and $24\ \mu\text{m}$ fluxes. Another example of an observational manifestation of the evolution of hydrocarbon dust that we have considered here could be variations in the UV peak in the interstellar extinction curve [75], which is often associated with differences in the number of small hydrocarbon dust grains. Our model can be used to describe the evolution of the dust component not only of the ISM and large star-forming complexes, but also in so-called infrared bubbles observed around HII regions, and also in planetary nebulae and supernova remnants. The relationship between the evolution of dust in the ISM and its size distribution and the properties of its IR emission will be considered in a future paper.

Our described model for the evolution of dust is not the only one possible. For example, Chiar et al. [34] have considered another sequence in which, after their formation in evolved stars, hydrocarbon dust grains are predominantly aromatic, and form aliphatic mantles in the ISM as a result of bombardment by H atoms. It was noted in [76] that this is possible in molecular clouds, where aliphatic mantles grow on dust grains due to the accretion of hydrogen atoms. However, in diffuse media, we should observe the situation we have

considered — large dust grains possessing an aliphatic core surrounded by an aromatic envelope and fully aromatic small dust grains.

6. ACKNOWLEDGEMENTS

We thank the referee for valuable comments and corrections, E. Micelotta for consultations about the sputtering of PAHs, and V. Akimkin for useful advice and his interest in these studies. This work was partially supported by the Russian Foundation for Basic Research (grants 13-02-00640, 14-02-31456, 15-02-06204), a grant of the President of the Russian Federation (MK-4536.2015.2), the “Dinastiya” Foundation, and the Italian Ministero dell’Universita e della Ricerca.

-
1. A. Leger and J. L. Puget, *Astron. Astrophys.* **137**, L5 (1984).
 2. L. J. Allamandola, A. G. G. M. Tielens, and J. R. Barker, *Astrophys. J. Lett.* **290**, L25 (1985).
 3. W. W. Duley and D. A. Williams, *Mon. Not. R. Astron. Soc.* **196**, 269 (1981).
 4. A. P. Jones, L. Fanciullo, M. Köhler, L. Verstraete, V. Guillet, M. Bocchio, and N. Ysard, *Astron. Astrophys.* **558**, A62 (2013).
 5. S. Kwok and Y. Zhang, *Nature (London)* **479**, 80 (2011).
 6. K.-W. Chan, T. L. Roellig, T. Onaka, M. Mizutani, K. Okumura, I. Yamamura, T. Tanabé, H. Shibai, T. Nakagawa, and H. Okuda, *Astrophys. J.* **546**, 273 (2001); astro-ph/0008335.
 7. A. Li and V. T. Draine, *Astrophys. J. Lett.* **760**, L35 (2012), 1210.6558.
 8. S. Kwok and Y. Zhang, *Astrophys. J.* **771**, 5 (2013), 1304.7629.
 9. J. D. T. Smith, B. T. Draine, D. A. Dale, J. Moustakas, R. C. Kennicutt, Jr., G. Helou, L. Armus, H. Roussel, K. Sheth, G. J. Bendo, et al., *Astrophys. J.* **656**, 770 (2007); astro-ph/0610913.
 10. F. Galliano, E. Dwek, and P. Charnial, *Astrophys. J.* **672**, 214 (2008); arXiv: 0708.0790.
 11. B. T. Draine, D. A. Dale, G. Bendo, K. D. Gordon, J. D. T. Smith, L. Armus, C. W. Engelbracht, G. Helou, R. C. Kennicutt, Jr., A. Li, et al., *Astrophys. J.* **663**, 866 (2007); arXiv:astro-ph/0703213.

12. K. D. Gordon, C. W. Engelbracht, G. H. Rieke, K. A. Misselt, J.-D. T. Smith, and R. C. Kennicutt, Jr., *Astrophys. J.* **682**, 336 (2008); arXiv: 0804.3223.
13. M. S. Khramtsova, D. S. Wiebe, P. A. Boley, and Y. N. Pavlyuchenkov, *Mon. Not. R. Astron. Soc.* **431**, 2006 (2013); arXiv: 1302.4837.
14. Y. N. Pavlyuchenkov, M. S. Kirsanova, and D. S. Wiebe, *Astron. Rep.* **57**, 573 (2013).
15. D. S. Wiebe, M. S. Khramtsova, O. V. Egorov, and T. A. Lozinskaya, *Astron. Lett.* **40**, 278 (2014).
16. M. S. Khramtsova, D. S. Wiebe, T. A. Lozinskaya, and O. V. Egorov, *Mon. Not. R. Astron. Soc.* **444**, 757 (2014); arXiv: 1407.8307.
17. J. D. Slavin, E. Dwek, and A. P. Jones, *Astrophys. J.* **803**, 7 (2015), 1502.00929.
18. N. V. Voshchinnikov and T. Henning, *Astron. Astrophys.* **517**, A45 (2010), 1004.0967.
19. L. Pagani, J. Steinacker, A. Bacmann, A. Stutz, and T. Henning, *Science* **329**, 1622 (2010); arXiv: 1110.4180.
20. K. M. Sandstrom, A. D. Bolatto, B. T. Draine, C. Bot, and S. Stanimirović, *Astrophys. J.* **715**, 701 (2010); arXiv: 1003.4516.
21. C. W. Engelbracht, K. D. Gordon, G. H. Rieke, M. W. Werner, D. A. Dale, and W. B. Latter, *Astrophys. J. Lett.* **628**, L29 (2005); astro-ph/0506214.
22. L. Boschman, S. Cazaux, M. Spaans, R. Hoekstra, and T. Schlathölter, arXiv: 1504.08276 (2015).
23. J. Y. Seok, H. Hirashita, and R. S. Asano, *Mon. Not. R. Astron. Soc.* **439**, 2186 (2014); arXiv: 1401.3943.
24. C. Cecchi-Pestellini, S. Casu, G. Mulas, and A. Zonca, *Astrophys. J.* **785**, 41 (2014).
25. E. R. Micelotta, A. P. Jones, and A. G. G. M. Tielens, *Astron. Astrophys.* **510**, A36 (2010); arXiv: 0910.2461.
26. V. Mennella, G. M. Muñoz-Caro, R. Ruiterkamp, W. A. Schutte, J. M. Greenberg, J. R. Brucato, and L. Colangeli, *Astron. Astrophys.* **367**, 355 (2001).
27. F. W. Smith, *J. Appl. Phys.* **55**, 764 (1984).
28. S. Iida, T. Ohtaki, and T. Seki, in *Proceedings of the AIP Conference on Optical Effects in Amorphous Semiconductors*, AIP Conf. Proc. **120**, 258 (1984).
29. J. M. Greenberg, A. Li, C. X. Mendoza-Gomez, W. A. Schutte, P. A. Gerakines, and M. de Groot, *Astrophys. J. Lett.* **455**, L177 (1995).

30. W. W. Duley, *Astrophys. J.* **553**, 575 (2001).
31. E. Dartois, G. M. Muñoz-Caro, D. Deboffle, and L. d'Hendecourt, *Astron. Astrophys.* **423**, L33 (2004).
32. E. Dartois and G. M. Muñoz-Caro, *Astron. Astrophys.* **476**, 1235 (2007).
33. T. Pino, E. Dartois, A.-T. Cao, Y. Carpentier, T. Chamaillé, R. Vasquez, A. P. Jones, L. D'Hendecourt, and P. Bréchnignac, *Astron. Astrophys.* **490**, 665 (2008).
34. J. E. Chiar, A. G. G. M. Tielens, A. J. Adamson, and A. Ricca, *Astrophys. J.* **770**, 78 (2013).
35. E. R. Micelotta, A. P. Jones, and A. G. G. M. Tielens, *Astron. Astrophys.* **510**, A37 (2010); arXiv: 0912.1595.
36. E. R. Micelotta, A. P. Jones, and A. G. G. M. Tielens, *Astron. Astrophys.* **526**, A52 (2011); arXiv: 1012.1599.
37. M. Bocchio, E. R. Micelotta, A.-L. Gautier, and A. P. Jones, *Astron. Astrophys.* **545**, A124 (2012).
38. A. G. G. M. Tielens, C. F. McKee, C. G. Seab, and D. J. Hollenbach, *Astrophys. J.* **431**, 321 (1994).
39. L. Serra Díaz-Cano and A. P. Jones, *Astron. Astrophys.* **492**, 127 (2008).
40. A. P. Jones, A. G. G. M. Tielens, and D. J. Hollenbach, *Astrophys. J.* **469**, 740 (1996).
41. H. Hirashita and H. Yan, *Mon. Not. R. Astron. Soc.* **394**, 1061 (2009), 0812.3451.
42. H. Hirashita, *Mon. Not. R. Astron. Soc.* **407**, L49 (2010), 1006.2187.
43. T. Birnstiel, PhD Thesis (2011).
44. A. P. Jones, *Astron. Astrophys.* **540**, A1 (2012).
45. A. P. Jones, *Astron. Astrophys.* **540**, A2 (2012).
46. A. P. Jones, *Astron. Astrophys.* **542**, A98 (2012).
47. T. Allain, S. Leach, and E. Sedlmayr, *Astron. Astrophys.* **305**, 602 (1996).
48. W. W. Duley, V. I. Grishko, J. Kenel, G. Lee-Dadswell, and A. Scott, *Astrophys. J.* **626**, 933 (2005).
49. M. A. Tamor and S. N. Wu, *J. Appl. Phys.* **67**, 1007 (1990).
50. A. P. Jones, *Mon. Not. R. Astron. Soc.* **247**, 305 (1990).
51. Y. A. Gruzdkov, K. Watanabe, K. Sawabe, and Y. Matsumoto, *Chem. Phys. Lett.* **227**, 243 (1994).
52. A. R. Welch and D. L. Judge, *J. Chem. Phys.* **57**, 286 (1972).

53. A. P. Jones, *Astron. Astrophys.* **545**, C2 (2012).
54. M. E. Adel, O. Amir, R. Kalish, and L. C. Feldman, *J. Appl. Phys.* **66**, 3248 (1989).
55. K. A. K. Gadallah, H. Mutschke, and C. Jäger, *Astron. Astrophys.* **528**, A56 (2011).
56. H. W. Jochims, E. Ruhl, H. Baumgartel, S. Tobita, and S. Leach, *Astrophys. J.* **420**, 307 (1994).
57. J. Zhen, P. Castellanos, D. M. Paardekooper, H. Linnartz, and A. G. G. M. Tielens, arXiv: 1411.7230 (2014).
58. M. Nic, J. Jirat, and B. Kosata, *IUPAC Compendium of Chemical Terminology (Gold Book)*, online version (2012).
59. A. Li and J. I. Lunine, *Astrophys. J.* **594**, 987 (2003); astro-ph/0311070.
60. V. T. Draine and A. Li, *Astrophys. J.* **551**, 807 (2001); astro-ph/0011318.
61. S. Z. D. Cheng, *Handbook of Thermal Analysis and Calorimetry*, Volume 3: *Applications to Polymers and Plastics* (Elsevier Science B.V., Amsterdam, 2002).
62. W. Hurler, M. Pietralla, and A. Hammerschmidt, *Diamond Relat. Mater.* **4**, 954 (1995).
[http://libgen.org/scimag/index.php?s=10.1016/0925-9635\(94\)00259-2](http://libgen.org/scimag/index.php?s=10.1016/0925-9635(94)00259-2)
63. L. Verstraete, A. Leger, L. D'Hendecourt, D. Defourneau, and O. Dutuit, *Astron. Astrophys.* **237**, 436 (1990).
64. J. C. Weingartner and B. T. Draine, *Astrophys. J. Suppl. Ser.* **134**, 263 (2001); astro-ph/9907251.
65. J. D. Slavin, A. P. Jones, and A. G. G. M. Tielens, *Astrophys. J.* **614**, 796 (2004).
66. V. V. Akimkin, M. S. Kirsanova, Y. N. Pavlyuchenkov, and D. S. Wiebe, *Mon. Not. R. Astron. Soc.* **449**, 440 (2015); arXiv: 1502.06865.
67. N. F. Mott and H. S. W. Massey, *The Theory of Atomic Collisions* (Clarendon, Oxford, 1949).
68. D. Joy, *Scanning* **17**, 270 (1995).
69. J. F. Ziegler, J. P. Biersack, and U. Littmark, in *The Stopping and Range of Ions in Matter* (Pergamon, New York, 1985).
70. B. T. Draine and E. E. Salpeter, *Astrophys. J.* **231**, 77 (1979).
71. J. S. Mathis, P. G. Mezger, and N. Panagia, *Astron. Astrophys.* **128**, 212 (1983).
72. J. Zhen, P. Castellanos, D. M. Paardekooper, N. Ligterink, H. Linnartz, L. Nahon, S. Joblin, and A. G. G. M. Tielens, *Astrophys. J. Lett.* **804**, L7 (2015); arXiv: 1505.00576.
73. J. S. Mathis, W. Rumpl, and K. N. Nordsieck, *Astrophys. J.* **217**, 425 (1977).

74. H. Yan, A. Lazarian, and V. T. Draine, *Astrophys. J.* **616**, 895 (2004), astro-ph/0408173.
75. E. L. Fitzpatrick and D. Massa, *Astrophys. J.* **307**, 286 (1986).
76. A. P. Jones, N. Ysard, M. Kohler, L. Fanciullo, M. Bocchio, E. Micelotta, L. Verstraete, and V. Guillet, *Faraday Discuss.* **168**, 313 (2014).
77. K. R. G. Roberts, K. T. Smith, and P. J. Sarre, *Mon. Not. R. Astron. Soc.* **421**, 3277 (2012); arXiv: 1201.3542.
78. K. Sellgren, M. W. Werner, J. G. Ingalls, J. D. T. Smith, T. M. Carleton, and C. Joblin, *Astrophys. J. Lett.* **722**, L54 (2010); arXiv: 1009.0539.
79. J. Cami, J. Bernard-Salas, E. Peeters, and S. E. Malek, *Science* **329**, 1180 (2010).
80. O. Berné and A. G. G. M. Tielens, *Proc. Nat. Acad. Sci.* **109**, 401 (2012); arXiv: 1111.0839.
81. S. Kendrew, R. Simpson, E. Bressert, M. S. Povich, R. Sherman, C. J. Lintott, T. P. Robitaille, K. Schawinski, and G. Wolf-Chase, *Astrophys. J.* **755**, 71 (2012); arXiv: 1203.5486.
82. R. J. Simpson, M. S. Povich, S. Kendrew, C. J. Lintott, E. Bressert, K. Arvidsson, C. Cyganowski, S. Maddison, K. Schawinski, R. Sherman, et al., *Mon. Not. R. Astron. Soc.* **424**, 2442 (2012); arXiv: 1201.6357.
83. V. Ossenkopf and T. Henning, *Astron. Astrophys.* **291**, 943 (1994).
84. H. Koyama and S.-i. Inutsuka, *Astrophys. J. Lett.* **564**, L97 (2002); astro-ph/0112420.
85. S. A. Khoperskov, E. O. Vasiliev, A. V. Khoperskov, and V. N. Lubimov, *J. Phys.: Conf. Ser.* **510**, 012011 (2014).
86. A. Sakata, S. Wada, T. Tanabe, and T. Onaka, *Astrophys. J. Lett.* **287**, L51 (1984).
87. R. W. Russell, V. T. Soifer, and K. M. Merrill, *Astrophys. J.* **213**, 66 (1977).
88. K. Sellgren, M. W. Werner, and H. L. Dinerstein, *Astrophys. J. Lett.* **271**, L13 (1983).
89. A. Li and V. T. Draine, *Astrophys. J.* **554**, 778 (2001), astro-ph/0011319.
90. Y. N. Pavlyuchenkov, D. S. Wiebe, V. V. Akimkin, M. S. Khramtsova, and T. Henning, *Mon. Not. R. Astron. Soc.* **421**, 2430 (2012), 1201.0642.
91. B. T. Draine and A. Li, *Astrophys. J.* **657**, 810 (2007), astro-ph/0608003.
92. B. T. Draine, *Astrophys. J. Suppl. Ser.* **36**, 595 (1978).
93. F. Boulanger, A. Abergel, J. P. Bernard, D. Cesarsky, J. L. Puget, W. T. Reach, C. Ryter, C. J. Cesarsky, M. Sauvage, D. Tran, et al., in *Proceedings of the Star Formation with the Infrared Space Observatory*, Ed. by J. Yun and L. Liseau, Vol. 132 of Astronomical Society of the Pacific Conference Series (ASP, 1998), p. 15.

94. M. H. Stockett, H. Zettergren, L. Adoui, J. D. Alexander, U. BÄ'rziĆš, T. Chen, M. Gatchell, N. Haag, B. A. Huber, P. Hvelplund, et al., *Phys. Rev. A* **89**, 032701 (2014).
95. M. J. Puska and R. M. Nieminen, *Phys. Rev. A* **47**, 1181 (1993).
96. M. J. Puska and R. M. Nieminen, *Phys. Rev. B* **27**, 6121 (1983).
97. A. Omont, *Astron. Astrophys.* **164**, 159 (1986).
98. T. Chen, M. Gatchell, M. H. Stockett, J. D. Alexander, Y. Zhang, P. Rousseau, A. Domaracka, S. Maclot, R. Delaunay, L. Adoui, et al., *J. Chem. Phys.* **140**, 224306 (2014).
99. J. Postma, R. Hoekstra, A. G. G. M. Tielens, and T. Schlathölter, *Astrophys. J.* **783**, 61 (2014).
100. Y. B. Zel'dovich and Y. P. Raizer, *Physics of Shock Waves and High-Temperature Hydrodynamic Phenomena* (Nauka, Moscow, 1966; Academic Press, New York, 1966, 1967).
101. C. Boersma, C. W. Bauschlicher, Jr., A. Ricca, A. L. Mattioda, J. Cami, E. Peeters, F. Sanchez de Armas, G. Puerta Saborido, D. M. Hudgins, and L. J. Allamandola, *Astrophys. J. Suppl. Ser.* **211**, 8 (2014).
102. E. Peeters, N. L. Martín-Hernández, F. Damour, P. Cox, P. R. Roelfsema, J.-P. Baluteau, A. G. G. M. Tielens, E. Churchwell, M. F. Kessler, J. S. Mathis, et al., *Astron. Astrophys.* **381**, 571 (2002).
103. D. A. Beintema, M. E. van den Ancker, F. J. Molster, L. B. F. M. Waters, A. G. G. M. Tielens, C. Waelkens, T. de Jong, T. de Graauw, K. Justtanont, I. Yamamura, et al., *Astron. Astrophys.* **315**, L369 (1996).
104. W. T. Reach, J. Rho, A. Tappe, T. G. Pannuti, C. L. Brogan, E. B. Churchwell, M. R. Meade, B. Babler, R. Indebetouw, and B. A. Whitney, *Astron. J.* **131**, 1479 (2006); astro-ph/0510630.
105. S. C. Madden, F. Galliano, A. P. Jones, and M. Sauvage, *Astron. Astrophys.* **446**, 877 (2006); astro-ph/0510086.
106. B. O'Halloran, S. Satyapal, and R. P. Dudik, *Astrophys. J.* **641**, 795 (2006); arXiv:astro-ph/0512404.
107. J. Y. Seok, H. Hirashita, and R. S. Asano, *Mon. Not. R. Astron. Soc.* **439**, 2186 (2014); arXiv:1401.3943.
108. C. F. Bohren and D. R. Huffman, *Absorption and Scattering of Light by Small Particles* (Wiley, New York, 1983).
109. B. T. Draine and H. M. Lee, *Astrophys. J.* **285**, 89 (1984).

110. V. Zubko, E. Dwek, and R. G. Arendt, *Astrophys. J. Suppl. Ser.* **152**, 211 (2004), astro-ph/0312641.
111. J. S Weingartner and V. T. Draine, *Astrophys. J.* **548**, 296 (2001), astro-ph/0008146.
112. M. Compiegne, L. Verstraete, A. Jones, J.-P. Bernard, F. Boulanger, N. Flagey, J. le Bourlot, D. Paradis, and N. Ysard, *Astron. Astrophys.* **525**, A103 (2011); 1010.2769.
113. T. Lejeune, F. Cuisinier, and R. Buser, *Astron. Astrophys. Suppl. Ser.* **125**, 229 (1997); astro-ph/9701019.
114. C. Leitherer, D. Schaerer, J. D. Goldader, R. M. G. Delgado, C. Robert, D. F. Kune, D. F. de Mello, D. Devost, and T. M. Heckman, *Astrophys. J. Suppl. Ser.* **123**, 3 (1999); astro-ph/9902334.
115. F. S Gillett, W. J. Forrest, and K. M. Merrill, *Astrophys. J.* **183**, 87 (1973).
116. J. M. Greenberg, *Interstellar Grains* (Univ. Chicago Press, Chicago, 1968), p. 221.
117. B. T. Draine and A. Li, *Astrophys. J.* **551**, 807 (2001); astro-ph/0011318.
118. Y. N. Pavlyuchenkov, D. S. Wiebe, V. V. Akimkin, M. S. Khramtsova, and T. Henning, *Mon. Not. R. Astron. Soc.* **421**, 2430 (2012), 1201.0642.
119. D. Massa and B. Savage, in *Interstellar Dust, Proceedings of the IAU Symposium No. 135*, Ed. by L. J. Allamandola and A. G. G. M. Tielens, *IAU Symp. Proc.* **135**, 3 (1989).
120. N. V. Voshchinnikov, V. B. Il'in, and T. Henning, *Astron. Astrophys.* **429**, 371 (2005); astro-ph/0409457.
121. P. Pilleri, S. Joblin, F. Boulanger, and T. Onaka, arXiv: 1502.04941 (2015).
122. T. I. Mori, T. Onaka, I. Sakon, D. Ishihara, T. Shimonishi, R. Ohsawa, and A. C. Bell, *Astrophys. J.* **784**, 53 (2014); arXiv: 1401.7879.
123. C. Joblin, A. G. G. M. Tielens, L. J. Allamandola, and T. R. Geballe, *Astrophys. J.* **458**, 610 (1996).
124. E. Churchwell, M. S. Povich, D. Allen, M. G. Taylor, M. R. Meade, B. L. Babler, R. Indebetouw, S. Watson, B. A. Whitney, M. G. Wolfire, et al., *Astrophys. J.* **649**, 759 (2006).
125. L. Deharveng, F. Schuller, L. D. Anderson, A. Zavagno, F. Wyrowski, K. M. Menten, L. Bronfman, L. Testi, C. M. Walmsley, and M. Wienen, *Astron. Astrophys.* **523**, A6 (2010); arXiv: 1008.0926.
126. L. D. Anderson, A. Zavagno, L. Deharveng, A. Abergel, F. Motte, P. Andre, J.-P. Bernard, S. Bontemps, M. Hennemann, T. Hill, et al., *Astron. Astrophys.* **542**, A10 (2012); arXiv:

1203.5721.

127. T. P. [Stecher and B. Donn, *Astrophys. J.* **142**, 1681 (1965).

APPENDIX A

COMPUTATION OF THE ENERGY TRANSFERRED TO A DUST GRAIN BY AN ION DUE TO FRICTION

The model assumes that an ion transfers an amount of energy to a a-C:H dust grain as it traverses one molecular layer. This energy can be estimated using the formula propose in [35] for molecular PAHs:

$$E_{\text{tr}}^0 = \int_{-s/2}^{s/2} \gamma(r_s) v_{\text{ion}} ds, \quad (\text{A1})$$

where s is the distance along the trajectory of a photon as a function of the angle θ between the layer and the ion trajectory:

$$s = \begin{cases} d/2 \cos \theta & \theta < \text{arcctg}(d/2a) \\ a/2 \sin \theta, & \theta > \text{arcctg}(d/2a) \\ \sqrt{d^2 + a^2}, & \theta = \text{arcctg}(d/2a) \end{cases} \quad (\text{A2})$$

Here, d and a are the thickness (4.31 Å [97]) and radius of a single layer of the molecular structure of the dust grains. The zero point is located at the center of the PAH, or, in our case, in the center of the layer.

The parameter r_s depends on the electron density n_0 as $(4/3\pi n_0)^{-1/3}$, and the electron density depends on the configuration of the molecules. It was proposed in [35] to use the following expression for the electron density, based on the computations of [95] for fullerene, but taking into account the different shape of PAHs:

$$n_0 = 0.15 \exp[-(s \cos \theta)^2 / 2.7]. \quad (\text{A3})$$

The parameter γ is calculated in terms of r_s :

$$\gamma(r_s) = \Gamma_0^{\text{ion}} \exp(-(r_s - 1.5)/R_2^{\text{ion}}) \quad (\text{A4})$$

with $R_2 = (2.28, 0.88, 0.90)$ and $\Gamma_0^{\text{ion}} = (0.310, 1.112, 0.690)$ for ions of hydrogen, helium, and carbon, respectively.

COMPUTATION OF THE ENERGY TRANSFERRED TO AN ATOM IN THE LATTICE DUE TO A COLLISION WITH AN INCIDENT PARTICLE

The maximum amount of energy $E_{\text{tr}}^{\text{max}}$ that an ion can transfer in a head-on collision with a carbon atom in the lattice is related to the kinetic energy of the ion through the coefficient γ , which can be calculated in terms of the masses of the colliding particles:

$$E_{\text{tr}}^{\text{max}} = \gamma E = \frac{4M_{\text{ion}}M_{\text{C}}}{(M_{\text{ion}} + M_{\text{C}})^2} E_0^{\text{ion}}, \quad (\text{B1})$$

where M_{ion} is the mass of the ion and M_{C} the mass of the carbon atom. Based on this expression, the minimum kinetic energy of an incident particle in order for it to be able to knock out an atom from the lattice with $T_{\text{crit}} = 7.5$ eV should be 26.8, 6 and 7.5 eV for H^+ , He^+ , and C^+ ions, respectively. According to [25], the interaction cross section $\sigma(E)$ per atom for ions with energies above the critical energy can be calculated as follows:

$$\begin{aligned} \sigma(E_0^{\text{ion}}) &= 4\pi a^{\text{scr}} Z_{\text{ion}} Z_{\text{C}} e^2 \frac{M_{\text{ion}}}{M_{\text{ion}} + M_{\text{C}}} s_n \times \\ &\times \frac{1-m}{m} \frac{1}{\gamma E_0^{\text{ion}}} \left(\left[\frac{E_{\text{crit}}^{\text{ion}}}{E_0^{\text{ion}}} \right]^{-m} - 1 \right) \end{aligned} \quad (\text{B2})$$

where a^{scr} is the screening length, Z_{ion} and Z_{C} are the charge numbers of the ion and carbon, e is the electron charge, s_n is the specific cross section for nuclear deceleration, and m is a parameter that depends on the energy through a relation taken from [69]. The mean energy transferred to the carbon atom is given by

$$\langle E_{\text{tr}}^{\text{elas}} \rangle = \frac{m}{1-m} \gamma \frac{(E_0^{\text{ion}})^{1-m} - (E_{\text{crit}}^{\text{ion}})^{1-m}}{(E_{\text{crit}}^{\text{ion}})^{-m} - (E_{\text{tr}}^{\text{max}})^{-m}} \quad (\text{B3})$$